Biophysical Chemistry, 47 (1993) 113–121
Elsevier Science Publishers B.V., Amsterdam

BIOCHE 01758

Helix propensity of Ala and Val: A free energy perturbation study

Yuto Komeiji [a], Nobuo Honda [b] and Ichiro Yamato [b,*]

[a] *Molecular Physics Section, Electrotechnical Laboratory, Agency of Industrial Science and Technology, 1-1-4 Umezono, Tsukuba-shi, Ibaraki 305 (Japan)*
[b] *Department of Biological Science and Technology, Science University of Tokyo, 2641 Yamazaki, Noda-shi, Chiba 278 (Japan)*

(Received 14 December 1992, accepted in revised form 4 February 1993)

Abstract

Difference in helix propensity between Ala and Val was examined by a molecular dynamics/free energy perturbation method. Simulations were based on a simple two state model of helix-coil transition. Val^{10} in an Ala based 17mer peptide ($Y^1K^2A^3A^4A^5A^6K^7A^8A^9V^{10}A^{11}K^{12}A^{13}A^{14}A^{15}A^{16}K^{17}$) used as the α-helical model, or in an extended trimer ($A^9V^{10}A^{11}$) used as the random coil model, was perturbed to Ala by a slow growth method. The computed $\Delta\Delta G$ (-1.27 ± 0.92 kcal/mol) reproduced semiquantitatively the experimental $\Delta\Delta G$ (-0.7 kcal/mol; Padmanabhan et al., *Nature* 344 (1990) 268). Inclusion of intraperturbed contributions was essential. Free energy component analysis showed that intra-perturbed interaction within Val^{10} contributed positive value to $\Delta\Delta G$ and that interaction between Lys^7 and Val^{10} contributed negative value. The latter dominated the former, which resulted in the larger helix propensity of Ala.

Keywords: Helix propensity; Free energy perturbation; Molecular dynamics simulation

1. Introduction

In recent years, the folding problem of polypeptides is recognized as the most important in the biological field. Thus a number of investigations have focused on the secondary structure formation of polypeptides, especially on the helix propensity of amino acids. Baldwin and his colleagues have done a systematic investigation on relative helix forming tendency of amino acid residues by using Ala-based synthetic peptides [1–4]. They drew conclusions that the helix propensity of an amino acid residue depends upon the context (sequence) and that conformational entropy and hydrophobic interactions likely play important roles.

The computer simulation has been demonstrated to be a powerful method in understanding biochemical phenomena, owing to the development of super computing techniques [5]. Such a technique should be useful in theoretical analysis of small peptides. It would be ideal if we could follow dynamics of peptides sufficiently long to sample the probability of appearance of the helix and random coil states by molecular dynamics

* To whom correspondence should be addressed.

simulation, but such simulation should take unrealistically long CPU time. Thus most molecular dynamics studies on helix stability are restricted to the unfolding step [6,7]. On the other hand, if the relative helix forming tendency of two different amino acid residues is discussed, free energy perturbation [8] must be a suitable method.

In this report we present results of free energy perturbation calculations on the relative helix forming tendency of Ala and Val residues in an Ala-based peptide. Our simulation is basically aimed at reproduction of an experiment by Padmanabhan et al. [2]. Applicability and limitation of the method to the study of helix propensity are discussed. Similar calculations on helix propensity have been extensively performed by Herman and his colleagues [9,10]. They investigated the effect of side chain rotation on helix propensity. In our present study we used free energy component analysis [11,12] in which free energy change is decomposed into contributions of residues and atoms. Thus a different aspect of the helix propensity is presented.

2. Methods

2.1. Assumption

Our calculation is based upon the following two state model of helix–coil transition.

$$\text{Helix} \xrightarrow{\Delta G} \text{Random coil} \qquad (1)$$

Experimentally, the free energy change (ΔG) is obtained from helix content f by eq. (2),

$$\Delta G = RT \ln\left(\frac{f}{1-f}\right) \qquad (2)$$

where R and T are the gas constant and absolute temperature, respectively. It is practically difficult to evaluate absolute ΔG by molecular dynamics/free energy perturbation method [8]. Nevertheless, it is possible to compare helix propensity of two amino acid residues (A and B) by assuming a thermodynamic cycle below.

$$\begin{array}{ccc} \text{Helix(A)} & \xrightarrow[\Delta G_A]{} & \text{Random coil(A)} \\ \Big\downarrow{\scriptstyle \Delta G_H} & & \Big\downarrow{\scriptstyle \Delta G_R} \\ \text{Helix(B)} & \xrightarrow[\Delta G_B]{} & \text{Random coil(B)} \end{array} \qquad (3)$$

The free energy changes associated with horizontal reactions (ΔG_A, ΔG_B) can be obtained by experimentation, and those associated with vertical reactions (ΔG_H, ΔG_R) by computer simulation. The vertical reactions correspond to unphysical replacement of amino acid residue A with B. Then, eq. (4) follows because the cycle (3) is closed.

$$\Delta\Delta G_{exp} \equiv \Delta G_A - \Delta G_B = \Delta G_H - \Delta G_R \equiv \Delta\Delta G_{comp} \qquad (4)$$

Thus the result by computation can be directly compared with that by experimentation. $\Delta\Delta G$ indicates the difference in helix forming tendency between A and B.

In this study, we analyzed a case where A denotes valine and B alanine. An experiment by Padmanabhan et al. [2] showed that $\Delta G_A = -0.02$ kcal/mol, $\Delta G_B = 0.69$ kcal/mol, and hence $\Delta\Delta G_{exp} = -0.70$ kcal/mol. This result indicated that Ala had a greater tendency to form helix in the peptide sequence they analyzed. Whether or not $\Delta\Delta G_{comp}$ can reproduce $\Delta\Delta G_{exp}$ is a criterion of feasibility of simulation.

2.2. Computational procedure

All simulations were performed with a program package of AMBER 3.0 Rev. A [13] and a locally modified version of it [12 and this work]. The AMBER all atom force field was employed [13,14]. Nonbonded interactions (electrostatic and van der Waals) between 1–4 pairs were divided by a factor of 2. We modified the GIBBS module to sample the intra-perturbed contributions in computing free energy change, which were neglected in the original program. The modified program, which can also carry out the free energy

component analysis [11], was used for free energy calculations. Only nonbonded contributions were considered in calculation of free energy changes, and contributions from covalent interactions were neglected.

The temperature was kept constant at 273 K by weak coupling to an external bath with a time constant of 0.2 ps [15]. A time step of 2 fs was used with SHAKE in molecular dynamics and free energy perturbation [16]. SHAKE was not used in energy minimization. The cut-off radius for nonbonded interactions was 10 Å. A dielectric constant of unity was used unless otherwise indicated.

We used a 17mer peptide of $Y^1K^2A^3A^4A^5A^6K^7A^8A^9V^{10}A^{11}K^{12}A^{13}A^{14}A^{15}A^{16}K^{17}$ for simulation of the α-helical model, following the experiment [2]. We employed an extended trimer model [9,17] for the random coil state ($A^9V^{10}A^{11}$; each number indicates the corresponding position in the 17mer sequence). Blocked termini were used for both peptide models [17].

The structure of the 17mer α-helix was generated as follows. First, three main chain atoms (N, C_α, C) of each residue were placed along a right-handed helix with a pitch of 1.5 Å and a radius of 2.3 Å, so that each turn contained 3.6 residues. Then H and O were added to N and C, respectively, so that they should form (i, $i+3$) hydrogen bonding (i is the sequential number of a residue). Side chain atoms were added by using EDIT module of AMBER. Then the 17mer was energy minimized in vacuo with a distance dependent dielectric (i.e. of r) until the norm of the gradient fell within 0.2 kcal/mol. The 17mer was placed in a sphere (radius = 20 Å) of TIP3P water [18] (920 molecules), H_β of Val^{10} being the center of the sphere. The water molecules were restricted within the sphere by imposing harmonic constraint force of 0.6 kcal/Å.

We first tried simulation of the trimer in a similar CAP water. The trimer stayed in the middle of the water in 50 ps simulations but not in 100 ps simulations (data not shown). Hence, we used a periodic box of water to solvate the trimer ($36.0 \times 26.6 \times 25.6$ Å^3; 684 water molecules), and the simulation of the trimer was performed under a constant pressure (1 atm) [15].

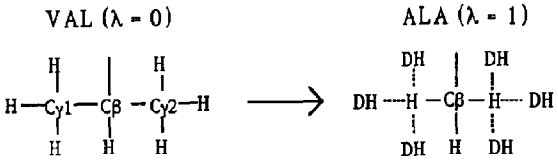

Fig. 1. The perturbation Val → Ala. In the Ala state (right), two hydrogens were connected to dummy hydrogens (DH). The dummy hydrogens had no nonbonded interactions with the system (van der Waals or electrostatic). The force constants for bonded interactions involving dummy hydrogens did not change during perturbation.

Val^{10} in the middle of each peptide was mutated to Ala by a slow growth method [19].

A simulation protocol described below was used. First, each solvated peptide was energy minimized with MIN module and equilibrated by molecular dynamics for 10 ps with MD module. Then Val^{10} ($\lambda = 0$; λ is the coupling parameter [8,19]) was perturbed to Ala ($\lambda = 1$). The dummy atoms and parameters were assigned according to the standard procedure [19] (Fig. 1). After forward simulation ($\lambda = 0 \rightarrow 1$) was completed, the system was equilibrated for 10 ps at $\lambda = 1$, and then reverse simulation ($\lambda = 1 \rightarrow 0$) was performed. Two cycles of simulations were performed for each peptide model. One way perturbation was completed in 50 ps in cycle 1 and in 100 ps in cycle 2.

Computation was carried out on an Apollo 9000/720 computer (Hewlett-Packard). A 1 ps simulation took 30 minutes of CPU time for the 17mer and 35 minutes for the trimer.

3. Results and discussion

3.1. Comparison of computational results with experiment

We first compared $\Delta\Delta G_{exp}$ and $\Delta\Delta G_{comp}$ (summarized in Tables 1 and 2).

$\Delta\Delta G_{comp}$ was -1.22 ± 0.30 kcal/mol in cycle 1 and -1.32 ± 0.96 kcal/mol in cycle 2. Both values were semiquantitatively close to $\Delta\Delta G_{exp}$ (-0.7 kcal/mol). Though the simulation time was longer in cycle 2, we saw no essential difference between cycles 1 and 2. We therefore aver-

aged the results of the two cycles. $\Delta\Delta G_{comp}$ thus obtained was -1.27 ± 0.92 kcal/mol.

$\Delta\Delta G_{comp}$ showed poorer agreement with $\Delta\Delta G_{exp}$ when intra-perturbed contributions were neglected (-1.69 kcal/mol in cycle 1 and -2.15 kcal/mol in cycle 2). In AMBER 3.0, the intra-perturbed contributions are always neglected because they could bring about large statistical noise [13]. Such neglect is reasonable when the perturbed group takes a similar conformation in the two systems compared (for instance, mutation in two liganded forms of a protein), because the intra-perturbed contributions should cancel out if double free energy difference $\Delta\Delta G$ is calculated. On the other hand, the perturbed group (Val^{10}) itself takes different conformations in the two peptide models examined in this study, and therefore calculation of intra-perturbed contributions was inevitable to obtain reasonable results.

3.2. Free energy component analysis

$\Delta\Delta G_{comp}$ was decomposed into contributions of different interactions (Table 3). The values were averaged over forward and reverse simulations of both cycles. We should note that free energy contribution of each residue depends on the path through which the perturbation was performed unless the perturbation time is infinite. Hence the discussion below is essentially qualitative rather than quantitative.

When total $\Delta\Delta G$ is considered, van der Waals contribution was large (-1.29 kcal/mol) while electrostatic contribution was small (0.03 kcal/mol), as expected from the nature of mutation Val → Ala. Intra-perturbed contribution (0.66 kcal/mol) and contribution of Lys^7 (-1.52 kcal/mol) were dominant. No other component seemed to contribute to $\Delta\Delta G$ significantly.

The intra-perturbed contribution of Val^{10} was decomposed into contributions from the interaction within the side chain and that within the main chain (Table 4). The intra-perturbed contribution to $\Delta\Delta G$ (0.66 kcal/mol) was mainly attributable to van der Waals contribution of the interaction between the main chain and the side chain (0.70 kcal/mol).

Thus replacement of Val^{10} with Ala stabilized Val^{10}–Lys^7 interaction in the α-helix but destabilized the main chain-side chain interaction within Val^{10}. Cancellation of these contributions resulted in the slightly larger helix propensity of Ala than that of Val. This observation suggests

Table 1

Summary of calculated free energy changes (Cycle 1, 50 ps perturbation) [a]

Model		$\Delta G_{forward}$ (kcal/mol)	$\Delta G_{reverse}$ [b] (kcal/mol)	$\Delta G_{average}$ (kcal/mol)
17mer	intra-perturbed	−6.52	−6.75	−6.63 (0.12) [c]
	rest	−2.07	−1.50	−1.79 (0.29)
	total	−8.60	−8.25	−8.43 (0.18)
Trimer	intra-perturbed	−7.22	−6.99	−7.11 (0.12)
	rest	−0.23	0.03	−0.10 (0.13)
	total	−7.45.	−6.95	−7.20 (0.25)
		$\Delta\Delta G_{comp}$	intra-perturbed	0.47 (0.16)
			rest	−1.69 (0.32)
			total	−1.22 (0.30)
		$\Delta\Delta G_{exp}$		−0.7

[a] Each simulation was 50 ps long.
[b] The sign of $\Delta G_{reverse}$ was reversed so that it could be compared directly with $\Delta G_{forward}$.
[c] Statistical error (standard deviation).

Table 2

Summary of calculated free energy changes (cycle 2, 100 ps perturbation) [a]

Model		$\Delta G_{forward}$ (kcal/mol)	$\Delta G_{reverse}$ [b] (kcal/mol)	$\Delta G_{average}$ (kcal/mol)
17mer	intra-perturbed	−6.29	−5.12	−5.71 (0.59)
	rest	−2.24	−1.64	−1.94 (0.30)
	total	−8.53	−6.77	−7.65 (0.88)
Trimer	intra-perturbed	−6.73	−6.36	−6.54 (0.19)
	rest	0.02	0.40	0.21 (0.19)
	total	−6.70	−5.96	−6.33 (0.38)
		$\Delta\Delta G_{comp}$	intra-perturbed	0.83 (0.62)
			rest	−2.15 (0.36)
			total	−1.32 (0.96)
		$\Delta\Delta G_{exp}$		−0.7

[a] Each simulation was 100 ps long.
[b,c] See legends for Table 1.

that helix propensity should be determined by a subtle balance of various contributions.

3.3. λ-Dependent solvation of Val^{10}

Several atoms gradually became dummy when Val^{10} is mutated to Ala (Fig. 1), but they did not disappear until the very end of forward simulation. The remaining dummy atoms could have caused an unnatural configuration of the system when λ became close to unity [20]. The dummy atoms were all exposed to the solvent in the present case, and if such an unnatural configuration occurred, it should cause an unnatural solvation pattern. Hence, we investigated a λ-dependent change of solvation of Val^{10}–C_β (Fig. 1), as expressed by the coordination number (number of water oxygen within 4 Å; Fig. 2). We per-

Table 3

Free energy component analysis

	ΔG_H [a]			ΔG_R [b]			$\Delta\Delta G$ (kcal/mol)		
	elc [c]	vdw [d]	sum	elc	vdw	sum	elc	vdw	sum
Intra-perturbed									
Val 10 [e]	−2.39	−3.78	−6.17	−2.40	−4.42	−6.82	0.01	0.64	0.66
	(0.53	0.22	0.63	0.53	0.24	0.33	0.75	0.32	0.71) [f]
Rest									
Solvent	−0.01	−1.14	−1.15	−0.04	−0.55	−0.59	0.03	−0.58	−0.55
	(0.02	0.26	0.26	0.06	0.91	0.96	0.05	0.95	0.99)
Ala 5	0.01	0.03	0.03	–	–	–	0.01	0.03	0.03
	(0.00	0.01	0.01	–	–	–	0.00	0.01	0.01)
Ala 6	0.07	−0.36	−0.29	–	–	–	0.07	−0.36	−0.29
	(0.03	0.14	0.12	–	–	–	0.03	0.14	0.12)
Lys 7	0.05	−1.57	−1.52	–	–	–	0.05	−1.57	−1.52
	(0.01	0.43	0.44	–	–	–	0.01	0.43	0.44)
Ala 8	0.00	0.17	0.17	–	–	–	0.00	0.17	0.17
	(0.02	0.02	0.02	–	–	–	0.02	0.02	0.02)
Ala 9	2.34	0.36	2.67	2.35	0.35	2.70	−0.01	0.01	0.00
	(0.01	0.08	0.09	0.02	0.10	0.12	0.03	0.12	0.14)
Ala 11	−2.00	0.02	−1.98	1.95	0.12	−1.83	−0.05	−0.10	−0.15
	(0.02	0.16	0.15	0.03	0.16	0.14	0.03	0.22	0.20)
Lys 12	−0.05	0.05	0.00	–	–	–	−0.05	0.05	0.00
	(0.01	0.01	0.01	–	–	–	0.01	0.01	0.01)
Ala 13	−0.02	0.08	0.07	–	–	–	−0.02	0.08	0.07
	(0.00	0.02	0.02	–	–	–	0.00	0.02	0.02)
Ala 14	−0.01	0.06	0.06	–	–	–	−0.01	0.06	0.06
	(0.00	0.02	0.02	–	–	–	0.00	0.02	0.02)
Ala 15	−0.00	0.01	0.00	–	–	–	−0.00	0.01	0.00
	(0.00	0.01	0.01	–	–	–	0.00	0.01	0.01)
Other	−0.01	0.04	0.03	0.02	0.23	0.25	−0.03	−0.19	−0.22
	(0.01	0.01	0.01	0.01	0.01	0.02	0.01	0.01	0.02)
Total	−2.01	−6.02	−8.04	−2.04	−4.73	−6.77	0.03	−1.29	−1.27
	(0.57	0.20	0.75	0.52	0.17	0.54	0.77	0.26	0.92)

[a] Free energy change in 17mer α-helix.
[b] Free energy change in trimer (random coil).
[c] Electrostatic contribution.
[d] Van der Waals contribution.
[e] The numbers correspond to the positions in the 17mer α-helix.
[f] Statistical error (standard deviation).

Table 4

Decomposition of intra-perturbed contribution

	ΔG_H (kcal/mol)			ΔG_R (kcal/mol)			$\Delta\Delta G$ (kcal/mol)		
	elc	vdw	sum	elc	vdw	sum	elc	vdw	sum
Within main chain [a]	–	–	–	–	–	–	–	–	–
Within side chain	−0.24	−1.17	−1.41	−0.24	−1.11	−1.34	0.00	−0.06	−0.06
	(0.00	0.10	0.10	0.00	0.02	0.02	0.00	0.10	0.10)
Between main and side chains	−2.16	−2.61	−4.76	−2.16	−3.31	−5.48	0.01	0.70	0.71
	(0.54	0.13	0.57	0.53	0.23	0.35	0.75	0.26	0.66)
Total	−2.39	−3.78	−6.17	−2.40	−4.42	−6.82	0.01	0.64	0.66
	(0.53	0.22	0.63	0.53	0.24	0.33	0.75	0.32	0.71) [b]

[a] Main chain atoms were N, HN, C_α, HA, C, and O. No nonbonded parameters changed in main chain in the perturbation Val → Ala; hence, there was no intra-main chain contribution.

[b] Standard deviation.

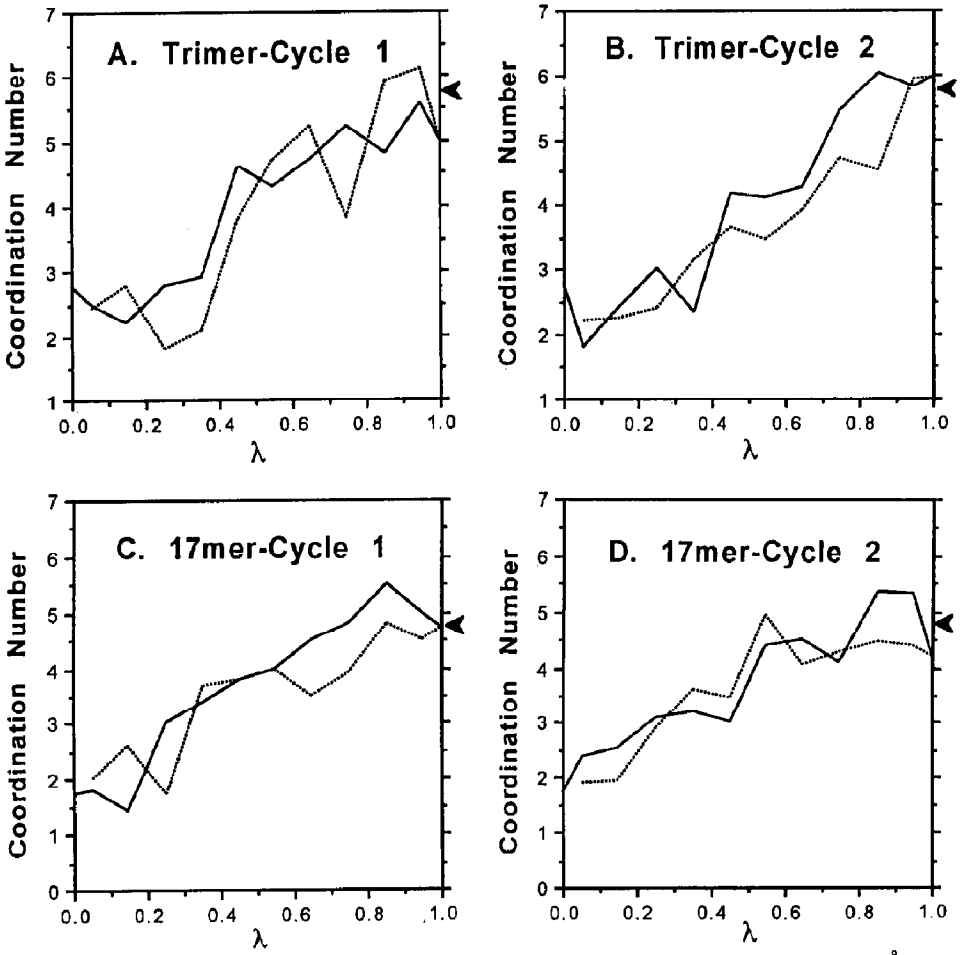

Fig. 2. λ-dependent change of solvation of Val^{10} shown by the number of water oxygens located within 4 Å of C_β-Val^{10}. The numbers were averaged over 0.1 reaction coordinate (λ). The arrows indicate the values calculated from trajectories of peptides without dummy atoms. Solid lines show forward simulations and dotted lines show reverse simulations.

formed molecular dynamics of each peptide without dummy atoms, namely with the usual Ala residue at position 10 (not shown). The average coordination number of C_β was 5.8 for the trimer and 4.8 for the 17mer (see the arrows in Fig. 2).

During perturbation the coordination number gradually increased as λ increased (Fig. 2), which was natural because Ala^{10} gradually replaced Val^{10}. When λ became almost unity, the coordination number of each peptide was similar to that of Ala without dummy hydrogens. Thus the artifact of dummy atoms was not prominent as far as solvation around the perturbed residue was concerned.

3.4. λ-Dependent conformation change of Val^{10}

It has been pointed out that free energy perturbation of floppy small peptides does not converge easily [21,22]. In our calculation, however, the hysteresis in the trimer was rather small (Tables 1, 2). We have found that hysteresis could become large when the conformation differed between forward and reverse simulations [12]. Conversely, the small hysteresis suggested the coincidence of the conformation in forward and reverse simulations.

To confirm this we compared λ-dependent conformation change of the trimer as illustrated by two main chain dihedral angles (ϕ, ψ) (Fig. 3). They indicated that almost similar conformations were sampled in both forward and reverse simulations in each cycle. We should not be too optimistic, however. The difference in ψ between cycles 1 and 2 suggested that such an agreement of conformations could be rather coincident (Figs. 3 B and D). Also, Pearlman and Kollman [20] pointed out that the hysteresis is simply the lower

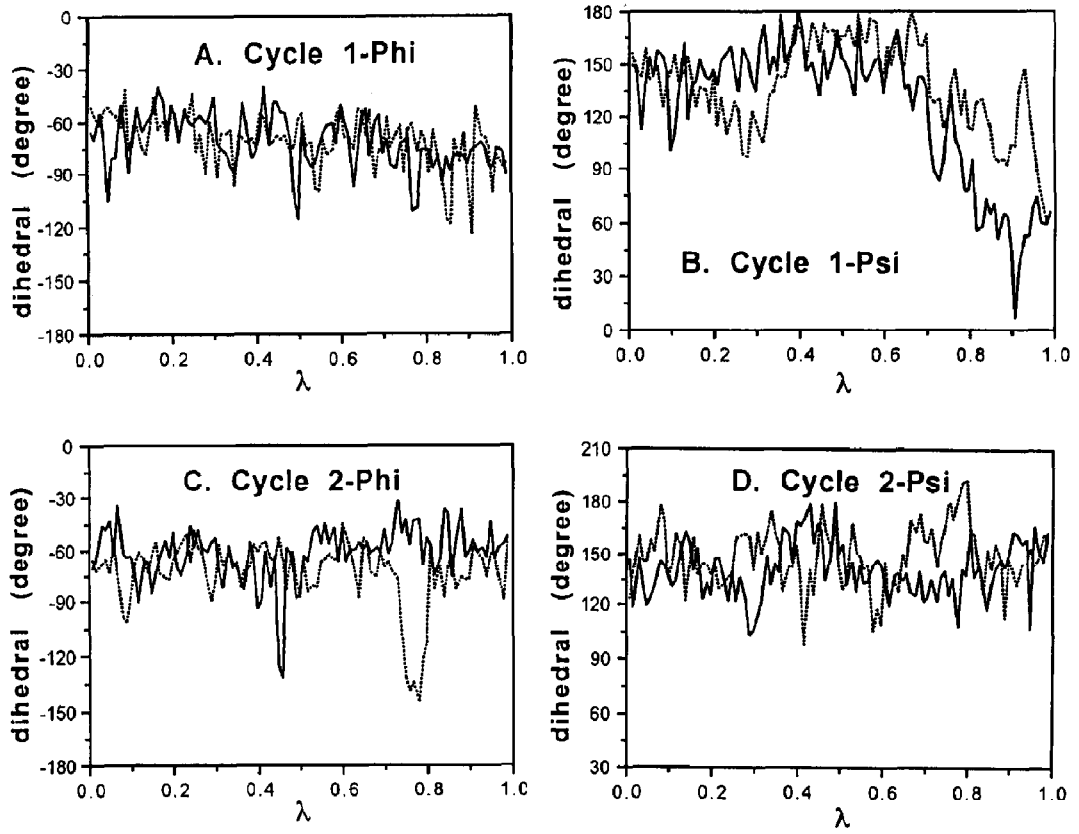

Fig. 3. λ-dependent conformation change of trimer shown by (ϕ, ψ) of Val^{10}. Solid lines show forward simulations and dotted lines show reverse simulations.

limit for the error. Anyway, average of forward and reverse simulations is fairly independent of the simulation protocol [22]. Therefore, even if our small hysteresis might be only fortuitous, the average ΔG of the trimer should be close to the true value.

In contrast to the trimer, the α-helical structure of the 17mer was stable throughout the simulation. Namely, (ϕ, ψ) of each residue was approximately (60°, 50°) and $(i, i+3)$ hydrogen bonds were marginally stable except in the terminal regions.

3.5. *Feasibility of the free energy perturbation method in estimation of the helix propensity*

Though our computational result agreed semiquantitatively with the experiment, some problems exist with respect to the two state model of helix–coil transition (eq. 1).

The first question is the feasibility of the extended trimer model for the random coil state. Is Val^{10} completely exposed to the solvent and interacting only with neighboring residues in the random coil state? We do not know the precise nature of the state. Probably the answer lies in the middle; Val^{10} may interact weakly with other residues while being mostly exposed to the solvent. Hence, the trimer model should have given an upper limit to the calculated free energy change [17], and it was reasonable that $\Delta\Delta G_{comp}$ somewhat overestimated $\Delta\Delta G_{exp}$. We used an extended peptide containing only three amino acid residues for the model of random coil state. A longer peptide model of the random coil should have brought about a similar result as far as an extended conformation is used [9], especially in the present case where the long-range electrostatic interactions had little contribution.

Secondly, there is an argument even on the helical state. Is the helix really α-helical? Shortly after we finished the analyses, Miick et al. [23] published a report on short Ala-based peptides similar to that we investigated here. Based on their FTIR and ESR experiments, they suggested that the helical state may be a mixture of α-helix and 3_{10}-helix and that the latter may dominate the former in solution. There is not a consensus on the structure of the helical state.

As mentioned above both simulation and experimentation have uncertainties, and our results are still preliminary. However, we have shown that simulation technique provides us with a theoretical tool to look into the minute problem of helix propensity.

Acknowledgments

We thank Mr. M. Uebayasi of National institute of bioscience and human technology and Mr. H. Katagiri of Electrotechnical laboratory for use of their facilities.

References

1 S. Marqusee, V.H. Robbins and R.L. Baldwin, Proc. Natl. Acad. Sci. USA 86 (1989) 5286.
2 S. Padmanabhan, S. Marqusee, T. Ridgeway, T.M. Laue and R. L. Baldwin, Nature 344 (1990) 268.
3 S. Padmanabhan and R.L. Baldwin, J. Mol. Biol. 219 (1991) 135.
4 A. Chakrabartty, J.A. Schellman and R.L. Baldwin, Nature, 351 (1991) 586.
5 M. Karplus and G.A. Petsko, Nature 347 (1990) 630.
6 J.M. DiCapua, S. Swaminathan and D.L. Beveridge, J. Am. Chem. Soc. 112 (1990) 6768.
7 J. Tirado-Rives and W.L. Jorgensen, Biochemistry 30 (1991) 3864.
8 D.L. Beveridge and F.M. DiCapua, Annu. Rev. Biophys. Biophys. Chem. 18 (1989) 431.
9 R.H. Yun and J. Hermans, Prot. Eng. 4 (1991) 761.
10 R.H. Yun, A. Anderson and J. Hermans, Proteins 10 (1991) 219.
11 N. Mizushima, D. Spellmeyer, S. Hirono, D.A. Pearlman and P.A. Kollman, J. Biol. Chem. 266 (1991) 11801.
12 Y. Komeiji, M. Uebayasi, J. Someya and I. Yamato, Prot. Eng. 5 (1992) 759.
13 G. Seibel, U.C. Singh, P.K. Weiner, J. Caldwell and P.A. Kollman, AMBER 3.0 Rev. A (University of California, San Francisco, CA, 1989).
14 S.J. Weiner, P.A., Kollman, D.T. Nguyen and D.A. Case, J. Comp. Chem. 7 (1986) 230.
15 H.J.C. Berendsen, J.P.M., Postma, W.F. van Gunsteren, A. DiNola, and J.R. Haak, J. Chem. Phys. 81 (1984) 3684.
16 J. Ryckaert, G. Ciccotti and H.J.C. Berendsen, J. Comp. Phys. 23 (1977) 327.
17 L.X. Dang, K.M. Merz, Jr. and P.A. Kollman, J. Am. Chem. Soc. 111 (1989) 8508.

18 W.L. Jorgensen, J. Chandrasekhar, M.D., Madura, R.W., Impey and M.L. Klein, J. Chem. Phys. 79 (1983) 926.
19 U.C. Singh, F.K. Brown, P.A. Bash and P.A. Kollman, J. Am. Chem. Soc. 109 (1987) 1607.
20 D.A. Pearlman and P.A. Kollman, J. Chem. Phys. 94 (1991) 4532.
21 M.J. Mitchell and J.A. McCammon, J. Comp. Chem. 12 (1991) 271.
22 J. Hermans, R.H. Yun and A.G. Anderson, J. Comp. Chem. 13 (1992) 430.
23 S.M. Miick, G.V. Martinez, W.R. Fiori, A.P. Todd and G.L. Millhauser, Nature 359 (1992) 653.